

CHARACTERISATION OF SIDE-CHAIN CONFORMATIONAL PREFERENCES IN A BIOLOGICALLY ACTIVE BUT UNFOLDED PROTEIN

STUART I. MATHIESON, CHRISTOPHER J. PENKETT,
AND LORNA J. SMITH

*Oxford Centre for Molecular Sciences, New Chemistry Laboratory,
University of Oxford, South Parks Road, Oxford OX1 3QT, England.*

A combination of experimental NMR $^3J_{\alpha\beta}$ coupling constant measurements and theoretical predictions from a statistical model for a random coil have been used to characterise the conformations of amino acid side-chains in an unfolded fibronectin binding protein. The statistical model uses the distribution of torsion angles in a data base of native folded protein structures to provide a description of the torsion angle populations of each residue in a random coil. For all but three of the residues studied a close agreement is observed between the experimental $^3J_{\alpha\beta}$ data and the model predictions (correlation coefficient 0.90; RMSD 0.70 Hz). In these cases the populations about the χ_1 torsion angles in the conformational ensemble defining the fibronectin binding protein are well described by those present in the protein data base. For Phe 69, Asp 92 and Asp 105 however significant deviations are observed between the predictions and experimental data. Each of these side-chains is found to be involved in persistent non-random structural features arising from clustering of hydrophobic groups or interactions between charged side-chains. The analysis demonstrates the detailed insight that can be provided into conformationally disordered states by combining experimental and theoretical approaches.

1 Introduction

Recently a number of proteins have been identified that are unfolded but biologically active under physiological conditions. One of these is a fibronectin binding protein from *Staphylococcal aureus*. This protein, an MSCRAMM (microbial surface components recognising adhesive matrix molecules), mediates the adhesion of bacterial cells to host tissue through binding to fibronectin.¹ High resolution nuclear magnetic resonance (NMR) studies of the fibronectin binding domain from this protein have demonstrated that its structural and dynamical characteristics at both a global and local level resemble those of most proteins under strongly denaturing conditions.^{2,3} Interestingly the binding domains of a number of other fibronectin binding MSCRAMMs also appear to be unfolded, circular dichroism studies identifying very little secondary structure in the proteins.^{4,5}

The unfolded nature of these fibronectin binding proteins has important consequences for their activity. Firstly it may enable hydrophobic groups, which are in general buried in globular proteins, as well as polar groups to be presented to fibronectin for binding.³ This could be significant in giving highly specific binding. The entropy cost of ordering the polypeptide chain will however reduce the

binding affinity allowing reversible binding in the presence of the high specificity.⁶⁻¹⁰ The lack of well defined structure may also be important in providing a mechanism for avoiding the immune system, the host being unable to produce tight binding antibodies for the unfolded chain.^{3,4} To understand these issues further a detailed characterisation of the proteins in both their free and fibronectin bound states is required. We have therefore extended our NMR studies of free *S. aureus* fibronectin binding protein. Previous work concentrated on NMR parameters that probe the polypeptide backbone.^{2,3} Here we report studies of the amino acid side-chains in the protein using $^3J_{\alpha\beta}$ coupling constants.

Defining the conformational properties of unfolded proteins is challenging as these states consist of ensembles of interconverting conformers.^{11, 12} Therefore when interpreting experimental data in structural terms, averaging of the experimental parameters across the conformational ensemble must be taken into account. One approach that has been very useful for understanding the conformational properties of unfolded proteins as well as non-native partly folded and denatured protein conformations uses a combination of experimental data and theoretical models for these states.^{12,13} The parameters predicted from the models provide a framework for interpreting the experimental data while the experimental data can be used to test the theoretical models. For aiding the interpretation of experimental NMR data for fibronectin binding protein (and also data for proteins under strongly denaturing conditions) the statistical model for a random coil has proved particularly successful.¹² An overview of this model is given in the next section.

2 The statistical model for a random coil

The model assumes that in a random coil the conformation of a given residue is independent of the neighbouring residues and there are no persistent non-local interactions (non-local in this context refers to interactions between residues that are not neighbours in the amino acid sequence). Even in a disordered state individual residues will however have local conformational preferences. For the main-chain in the simplest case these will be the low energy regions of the Ramachandran ϕ, ψ surface. In the statistical model the distribution of ϕ, ψ torsion angles in a data base of native folded protein structures is used to give a description of the main-chain torsion angle populations for each residue in a random coil.^{12,14,15} This assumes that by taking a large data set of structures the effects of non-local interactions present in individual structures will be averaged out. A similar approach has also been used for the side-chain χ_1 torsion angles, taking the protein data base χ_1 distributions as a representation of those in a random coil.¹⁶

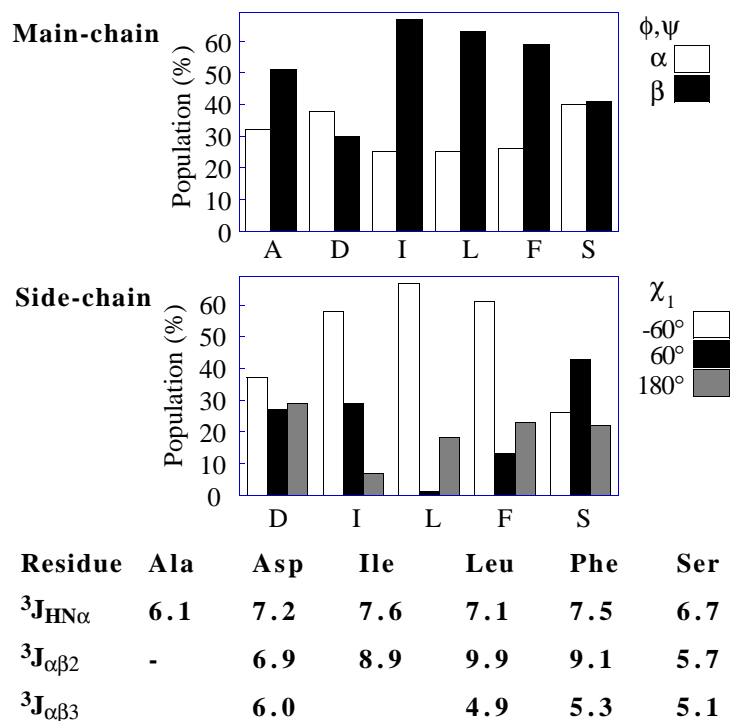


Figure 1. Examples of the percentage populations of the core α and β regions of ϕ, ψ space (as defined by Morris et al.¹⁸) and the three staggered χ_1 rotamers ($-60 \pm 30^\circ$, $60 \pm 30^\circ$, $180 \pm 30^\circ$) for different amino acids in a data base of 85 high resolution native folded protein structures.¹⁷ The values of the $^3J_{HN\alpha}$ and $^3J_{\alpha\beta}$ coupling constants ($^3J_{\alpha\beta 2}$, $^3J_{\alpha\beta 3}$) predicted from the data base distribution for a random coil are also given (in Hz). The data are from references 14 and 16. Only residues that are not in regions of recognised secondary structure (COIL residues) in the protein structures are used. Similar results, particularly for the polypeptide backbone, are obtained if all residues in the data base are considered.¹⁴ The torsion angles and side-chain β protons ($H\beta_2$ and $H\beta_3$) are defined according to the IUPAC-IUB conventions.¹⁹

For all amino acids (excluding glycine and proline) α and β main-chain ϕ, ψ conformations are favoured in the protein data base structures. In addition for all side-chain types (excluding glycine, alanine and proline) the staggered χ_1 rotamers of -60° , 60° and 180° are preferred. Significant differences are found, however, between the amino acids in the relative populations of these conformers (Figure 1).

These variations reflect the different characteristics of the amino acid side-chains.^{14,16,17} For example, isoleucine which has a β branched side-chain favours for steric reasons β rather than α main-chain ϕ, ψ conformers and $\chi_1 -60^\circ$ side-chain rotamers. In contrast serine, whose polar side-chain has the potential to form favourable electrostatic interactions with the main-chain amide group has a significant population of α main-chain and $\chi_1 60^\circ$ side-chain conformers. In these conformations the possibilities of main-chain to side-chain interactions are maximised. The distributions for specific amino acids are used in the model to give a description of the local properties of a random coil for a given polypeptide sequence in terms of statistical populations about specific torsion angles.

From the protein data base torsion angle distributions NMR parameters have been predicted for a random coil.¹⁴⁻¹⁶ In the case of main-chain $^3J_{\text{HN}\alpha}$ and side-chain $^3J_{\alpha\beta}$ spin-spin coupling constants (which probe ϕ and χ_1 respectively), these have been calculated directly from the torsion angle distributions using the Karplus relationship.²⁰ Rapid interconversion between conformers in a random coil is assumed, so the NMR parameters have been calculated as population weighted averages. For the prediction of NOE (nuclear Overhauser enhancement) intensities a Monte Carlo procedure has been used to generate ensembles of random coil conformers using the data base torsion angle distributions.¹⁵ From the distribution of interproton distances within these ensembles NOE intensities have been calculated.

Both the main-chain and side-chain coupling constants predicted for a random coil vary according to the amino acid type (Figure 1). These differences reflect the variations in torsion angle populations in the protein data base. Thus for $^3J_{\text{HN}\alpha}$ the largest values (7.6-7.7 Hz) are predicted for threonine, valine and isoleucine resulting from the preference of these amino acids for conformations in the β region of ϕ, ψ space. In contrast the smallest $^3J_{\text{HN}\alpha}$ coupling constants (5.9-6.1 Hz) are predicted for alanine (conformations with ϕ of approximately -60° favoured) and glycine (a wide range of ϕ, ψ torsion angles are populated). For $^3J_{\alpha\beta}$, for example, two very similar coupling constant values are predicted for serine ($^3J_{\alpha\beta 2}$ 5.7 Hz, $^3J_{\alpha\beta 3}$ 5.1 Hz) while the two values for leucine in contrast differ significantly ($^3J_{\alpha\beta 2}$ 9.9 Hz, $^3J_{\alpha\beta 3}$ 4.9 Hz; Figure 1). In the case of NOEs both sequential $\alpha\text{H-NH}(i, i+1)$ and $\text{NH-NH}(i, i+1)$ NOEs are predicted to be observed. This reflects the populations of both α and β conformers in a random coil. In addition a significant number of $(i, i+2)$ NOEs (particularly $\alpha\text{H-NH}(i, i+2)$) are predicted with variations in intensity according to the amino acid sequence.

Comparisons of the NMR parameters predicted from the statistical model with experimental data for short unstructured peptides and denatured proteins have shown in general a good agreement.^{14-16,21-23} Both the predicted variations in spin-spin coupling constants and the expected patterns of NOEs for a random coil have been

observed experimentally. For reduced lysozyme denatured in 8M urea, for example, a correlation coefficient of 0.89 is seen for the comparison of predicted and experimental $^3J_{\text{HN}\alpha}$ coupling constants.²³ It must be recognised however that the protein data base torsion angle distributions used in the model are only an approximation for the random coil energy surfaces. The protein torsion angle distributions may also contain biases from the potentials used in crystallographic refinement procedures. As further experimental data for unfolded protein conformations become available these issues should be able to be explored further and the statistical model modified accordingly. However, the random coil predictions from the current model do provide a important baseline for interpreting experimental data for disordered conformational ensembles. When comparisons of experimental data with the predictions show significant deviations for specific residues this provides clear evidence for identifying non-random persistent structural features. This is the approach that has been used for fibronectin binding protein.

3 Conformational characteristics of a fibronectin binding protein

The primary ligand binding site of fibronectin binding protein from *S. aureus* is a 130 residue sequence consisting of four repeats, D1 to D4 (Figure 2). Each repeat can bind fibronectin with low affinity and together (D1-D4) they form a high affinity binding domain.²⁴

```
D1 1  GQNSGNQSFE EDTEEDKPKY EQGG-NIVDI DFDSVPQIH
D2 39 GQNKGDQSFE EDTEKDKPKY EHGG-NIIDI DFDSVPHIH
D3 77 GFNKHTEIIE EDTNKDKPNY QFGGHNSVDF EEDTLPQVS
D4 116 GHNEGQQTIE EDTTT
```

Figure 2. Sequence alignment of D1, D2, D3 and D4 from *S. aureus* fibronectin binding protein (variant FnBPC²⁶) highlighting conserved residues in bold. The numbering used throughout the paper is that of the full D1-D4 binding domain as shown here.

Fragments with the full binding domain sequence (D1-D4) and the sequence of only the second and third domain (D2-D3) have been studied previously using high resolution NMR spectroscopy.^{2,3} Use of ^{15}N labelled samples and heteronuclear NMR techniques enabled the extraction and analysis of ^{15}N and ^1H chemical shifts, main-chain $^3J_{\text{HN}\alpha}$ coupling constants, NOE data and ^{15}N relaxation data. The average global dimensions of the molecule were also probed via NMR diffusion studies.²⁵ The analysis included comparison of the experimental data with

predictions from the statistical model for a random coil and also with experimental data for short unstructured model peptides and denatured proteins.

The conformational ensemble defining D1-D4 was found to have an average effective hydrodynamic radius (27Å), approximately 75% greater than that expected for a globular protein of 130 residues.³ Analysis of the NMR parameters that probe the local conformational properties showed a close overall agreement with predictions from the statistical model. Sequential NH-NH(i,i+1) and α H-NH(i,i+1) NOEs were observed throughout the D1-D4 sequence in accord with the predictions and 59 α H-NH(i,i+2) NOEs have been identified, 56 of which are predicted to be seen for a random coil.³ In the case of $^3J_{\text{HN}\alpha}$ coupling constants, the amino acid dependent variations expected for a random coil are observed. In addition the data for the protein enable more subtle sequence dependent variations in the random coil ϕ, ψ distributions, reflecting the characteristics of the preceding (i-1) residue, to be identified. The statistical model for a random coil has been extended to include these effects and an excellent agreement is seen between the model predictions and the experimental data for D1-D4 (correlation coefficient 0.92; RMSD 0.22 Hz).²

In three specific regions of the sequence, however, deviations were seen for the experimental NMR data from the parameters predicted from the statistical model and those predicted on the basis of parameters measured in short unstructured peptides. In each case persistent non-local interactions have been identified which are presumably responsible for biasing the torsion angle populations away from those predicted for a random coil.³ The first region involves the sequence EDT(E/N)KDK present in both D2 (Glu 49 to Lys 55) and D3 (Glu 87 to Lys 93). Here there is a persistent electrostatic interaction between glutamate and lysine side-chains with an i,i+4 separation. The second region involves residues Phe 98 to Gly 100 in D3. In this case there is an interaction between the phenylalanine aromatic ring and the amide group of Gly 100. In the third region hydrophobic clusters involving side-chain methyl and aromatic groups have been identified. The sequences involved here are IDFDSV in D1 and D2 (Ile 29 to Val 34 and Ile 67 to Val 72) and VDF in D3 (Val 104 to Phe 106).

4 Characterising side-chain conformations in a fibronectin binding protein

4.1 Experimental measurement

Studies of the full fibronectin binding domain, D1-D4, using homonuclear NMR techniques are hampered by the limited chemical shift dispersion observed in the NMR spectra of an unfolded protein. Therefore, for characterising the behaviour of

side-chains in fibronectin binding protein the work has concentrated on studying two shorter peptide fragments. In particular D2-D3, which has the sequence of the second and third fibronectin repeats (Gly 39 to Ser 115; Figure 2), and a 32 residue peptide from the D3 sequence (D3s; Glu 83 to Val 114) have been used. In D3s Asn 95 is changed to serine and Gln 113 to lysine (D3s sequence: EIIIEEDTNKDKP NYQFGGHNSVDFEEDTLPQV). D2-D3 was expressed in *E. coli* as described previously.³ The D3s peptide was synthesised on an Applied Biosystems 430A automated peptide synthesiser, using standard Fmoc methodology, and was purified by reverse phase HPLC. Samples of each of the peptides in aqueous solution for NMR studies were prepared using deuterated solvent with peptide concentrations of 1-2mM at pH 6. The NMR resonances of both the peptides have been assigned previously;^{3,27} an ¹⁵N labelled sample and heteronuclear NMR techniques were used for D2-D3. For D3s standard homonuclear techniques were employed, comparisons with the assignments for D2-D3 helping to resolve ambiguities arising from resonance overlap.²⁷ Due to the unfolded nature of the protein the main-chain structural NMR parameters for these shorter fragments are almost identical to those for the full D1-D4 sequence (excluding residues at the chain termini).^{3,27}

NMR experiments were run on the Oxford Centre for Molecular Sciences home built spectrometers operating at ¹H frequencies of 500.15 MHz and 600.20 MHz. For extraction of ³J_{αβ} coupling constants PE COSY (primitive exclusive correlation spectroscopy²⁸) experiments were performed at 283K for both peptides using 1024 t₁ increments and collecting 4K points with a β flip angle of 35°. In each case the resulting FID was zero filled twice in the direct dimension to 16K and both exponential and trapezoidal window functions were applied. In the indirect dimension, a sinebell square window function was used. The resulting digital resolution was approximately 0.5 Hz/point. From the spectra ³J_{αβ} coupling constants were extracted from the passive splittings for residues with two β protons (Figure 3). Pairs of ³J_{αβ} coupling constants could be measured for 13 residues in the D1-D4 sequence (Table 1). The data for different residues vary considerably; the two values for Ser 95 for example are very similar to each other (5.0, 5.2 Hz) and those for Leu 111 are significantly different (4.7, 10.2 Hz).

4.2 Analysis of the coupling constant data

The experimental ³J_{αβ} coupling constant data have been compared with the predictions for a random coil from the statistical model. As the NMR resonances of the β protons have not been stereospecifically assigned previously, in each case it was assumed that the β proton with the largest ³J_{αβ} coupling constant was Hβ2. This is the case when the population of the least sterically restricted χ₁ -60° rotamer is greater than that of the χ₁ 180° rotamer, a situation which is highly likely in an

unfolded protein.¹⁶ Tests of this assumption, using ^{13}C labelled samples and measuring heteronuclear coupling constants, are required however in the future.

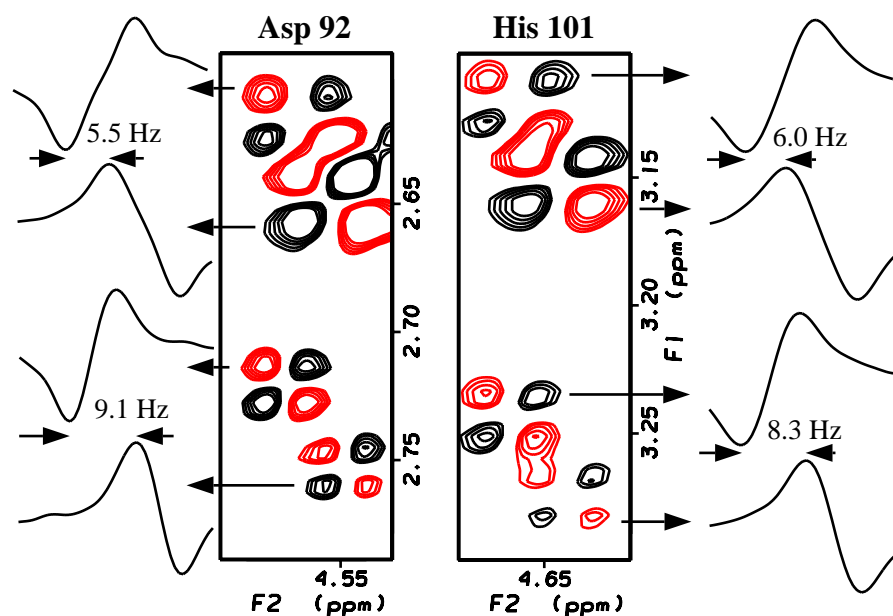


Figure 3. $\text{H}\alpha\text{-H}\beta$ cross peaks for Asp 92 and His 101 taken from the PE COSY spectrum of peptide D3s. Cross-sections through the cross peaks are shown which indicate how the $^3J_{\alpha\beta}$ coupling constants were extracted.

The differences between the coupling constant values for the two β protons ($|^3J_{\alpha\beta 2} - ^3J_{\alpha\beta 3}|$) are compared to simplify the analysis. A close agreement between the predictions and the experimental data is observed for ten of the residues (Figure 4; excluding Phe 69, Asp 92, Asp 105 correlation coefficient 0.90, RMSD 0.70 Hz). For these 10 residues therefore the χ_1 populations adopted in the ensemble of conformers in unfolded D1-D4 can be defined from the χ_1 distributions present in the native protein structures in the data base. Significant deviations are observed however for Phe 69, Asp 92 and Asp 105 between the experimental $^3J_{\alpha\beta}$ coupling constants and those predicted for a random coil (difference between predicted and experimental $|^3J_{\alpha\beta 2} - ^3J_{\alpha\beta 3}|$ greater than 2Hz). To understand these differences we compare these data with the conformational properties of D1-D4 identified from the previous NMR studies.^{2,3}

Table 1. Experimental $^3J_{\alpha\beta}$ coupling constant data for fibronectin binding protein recorded at pH 6 and 298K (error approximately ± 1 Hz). In each case the higher coupling constant value is listed first. The predictions from the statistical model for a random coil are also given.¹⁶

Residue	Experimental $^3J_{\alpha\beta}$ (Hz)	Predicted $^3J_{\alpha\beta 2}, ^3J_{\alpha\beta 3}$ (Hz)
Phe 47	7.9, 5.9	9.1, 5.3
Phe 69	8.1, 7.4	9.1, 5.3
His 81	8.0, 5.9	8.2, 5.5
Asp 88	7.6, 6.2	6.9, 6.0
Asp 92	9.1, 5.5	6.9, 6.0
Ser 95	5.2, 5.0	5.7, 5.2
Phe 98	8.8, 5.3	9.1, 5.3
His 101	8.3, 6.0	8.2, 5.5
Asn 102	7.8, 5.6	7.4, 5.8
Ser 103	5.5, 5.1	5.7, 5.2
Asp 105	8.7, 4.9	6.9, 6.0
Asp 109	7.2, 6.3	6.9, 6.0
Leu 111	10.2, 4.7	9.9, 5.0

Phe 69 is situated in a region of the sequence where a clustering of hydrophobic side-chains has been identified (Ile 67 to Val 92; see section 3 above). Previous characterisation of this cluster has shown that Phe 69 has a low main-chain $^3J_{\text{HN}\alpha}$ coupling constant value (5.6 Hz). In addition NOEs have been observed from the $\text{C}^{\gamma 2}\text{H}_3$ methyl group of Ile 67 to the backbone amides of Phe 69 and Asp 70. The NMR resonance of the Ile 67 $\text{C}^{\gamma 2}\text{H}_3$ methyl group is also significantly shifted upfield from the value observed in a short model peptides suggesting a close proximity of this methyl group in D1-D4 to the aromatic ring of Phe 69. It is therefore clear that there are non-local interactions within this region of the sequence. The coupling constant measurements enable the resulting changes in torsion angle populations for Phe 69 relative to those expected for a random coil to be defined. In particular there is an increased preference for main-chain α relative to β conformers and χ_1 rotamers of 60° or 180° relative to -60° . It is not clear from the current data, however, whether the changes to the side-chain χ_1 populations are caused by non-local interactions involving the side-chain itself or if they merely reflect changed side-chain preferences due to the perturbations in ϕ, ψ populations.

Asp 105 is also located in a region of the sequence where there is a hydrophobic cluster involving Val 104 and Phe 106, the aromatic and methyl side-chains of which have been shown to be in close proximity (see above). In addition, NOEs are observed between the side-chain methyl groups of Val 104 and the backbone amide

groups of Phe 106 and Glu 107. In this case the anomalous $^3J_{\alpha\beta}$ coupling constants observed for Asp 105 provide evidence showing that in this cluster the conformations that are favourable for the side-chain of Asp 105 to populate are also restricted. Here the coupling constant results show an increased preference for χ_1 rotamers of -60° or 180° .

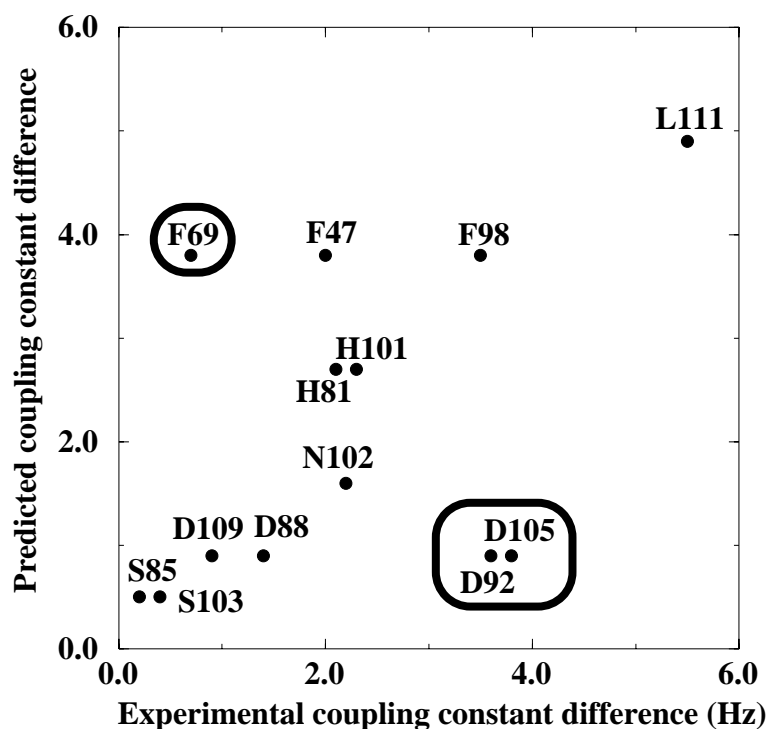


Figure 4. Comparison of the experimental $^3J_{\alpha\beta}$ coupling constants for fibronectin binding protein and the predictions from the statistical model for a random coil. The differences between the two coupling constants values for each residue are compared. The three residues which show significant deviations from the model are indicated (Phe 69, Asp 92, Asp 105; difference between predicted and experimental $|^3J_{\alpha\beta 2} - ^3J_{\alpha\beta 3}|$ greater than 2Hz).

Asp 92 is located within the EDTNKDK sequence found for residues Glu 87 to Lys 93 in which a persistent electrostatic interaction has been recognised occurring between the side-chains of Glu 87 and Lys 91. An $\alpha\text{H-NH}(i,i+3)$ NOE has been identified between Asn 90 and Lys 93 and a low $^3J_{\text{HN}\alpha}$ coupling constant recorded

for Lys 91 (5.7 Hz). These data suggest a favouring of α main-chain conformers relative to β for residues in the sequence Asn 90 to Lys 93. The results reported here show that the side-chain conformations populated by Asp 92 are also perturbed from those in a random coil. For Asp 92, as for Asp 105, the $^3J_{\alpha\beta}$ coupling constants show that there is an increased preference for χ_1 rotamers of -60° or 180° .

4.3 Conclusions

This study illustrates the value of the general approach we have developed, where experimental studies and theoretical models are combined in the characterisation of unfolded protein conformations. The combination of experimental $^3J_{\alpha\beta}$ coupling constant measurements and comparisons with predictions from the statistical model for a random coil have enabled the description of the ensemble of conformers defining fibronectin binding protein to be extended. For the local conformational properties, the description of the state in terms of statistical populations about specific torsion angles can now include the distributions about side-chain χ_1 torsion angles for a number of residues. The characterisation of the χ_1 preferences of Phe 69, Asp 92 and Asp 105 is of particular significance as studies of peptide fragments^{29,30} and sequence comparison between different fibronectin binding proteins¹ suggest that both the hydrophobic clusters and the charged sequence in which these residues are located have a functional role in fibronectin binding activity.³ Most importantly the hydrophobic sequences lie in the identified fibronectin binding site. The preferred conformations of these residues identified by the NMR analysis may therefore those selected from the ensemble of conformers for binding to fibronectin.

Acknowledgements

This is a contribution from the Oxford Centre of Molecular Sciences which is supported by the UK. Engineering and Physical Sciences Research Council, the Biotechnology and Biological Sciences Research Council and the Medical Research Council. LJS is a Royal Society University Research Fellow. We would like to thank Chris Dobson for his encouragement and support, Richard Smith for providing the D2-D3 sample, Jonathan Jones for help with recording the PE COSY spectra and Maureen Pitkeathly for synthesising the D3s peptide fragments.

References

1. J.M. Patti, B.L. Allen, M.J. McGavin and M. Höök, *Annu. Rev. Microbiol.* **48**, 585 (1994)

2. C.J. Penkett, C. Redfield, I. Dodd, J. Hubbard, D.L. McBay, D.E. Mossakowska, R.A.G. Smith, C.M. Dobson and L.J. Smith, *J. Mol. Biol.* **274**, 152 (1997)
3. C.J. Penkett, C. Redfield, J.A. Jones, I. Dodd, J. Hubbard, R.A.G. Smith, L.J. Smith and C.M. Dobson, *Biochemistry*, in press (1998)
4. K. House-Pompeo, Y. Xu, D. Joh, P. Speziale and M. Höök, *J. Biol. Chem.* **271**, 1379 (1996)
5. P. Speziale, D. Joh, L. Visai, S. Bozzini, K. House-Pompeo, M. Lindberg and M. Höök, *J. Biol. Chem.* **271**, 1371 (1996)
6. G.E. Schulz in *Molecular Mechanism of Biological Recognition*. Elsevier/North-Holland Biomedical Press. p79 (1979)
7. M.S. Searle et al, *J. Am. Chem. Soc.* **114**, 10697 (1992)
8. C.M. Dobson, *Current Biology* **3**, 530 (1993)
9. R.S. Spolar and M.T. Record, *Science* **263**, 777 (1994)
10. J.R. Altman et al, *Pac. Symp. Biocomp.* **3**, 473 (1998)
11. R.B. Gillespie and D. Shortle, *J. Mol. Biol.* **268**, 170 (1997)
12. L.J. Smith, K.M. Fiebig, H. Schwalbe and C.M. Dobson, *Folding and Design* **1**, R95 (1996)
13. L.J. Smith et al, *J. Mol. Biol.* **280**, 703 (1998)
14. L.J. Smith et al, *J. Mol. Biol.* **255**, 494 (1996)
15. K.M. Fiebig et al, *J. Phys. Chem.* **100**, 2661 (1996)
16. N.J. West and L.J. Smith, *J. Mol. Biol.* **280**, 867 (1998)
17. M.B. Swindells et al, *Nature Struct. Biol.* **2**, 596 (1995)
18. A.L. Morris et al, *Proteins: Struct. Funct. Genet.* **12**, 535 (1992)
19. IUPAC-IUB Commission on Biochemical Nomenclature, *J. Mol. Biol.* **52**, 1 (1970)
20. M. Karplus, *J. Chem. Phys.* **30**, 11 (1959)
21. K.A. Bolin et al, *J. Mol. Biol.* **262**, 443 (1996)
22. J.J. Yang et al, *Folding and Design* **1**, 473 (1996)
23. H. Schwalbe, K.M. Fiebig, M. Buck, J.A. Jones, S.B. Grimshaw, A. Spencer, S. Glaser, L.J. Smith and C.M. Dobson, *Biochemistry* **36**, 8977 (1997)
24. C. Signäs, G. Raucci, K. Jonsson, P.E. Lindgren, G.M. Anantharamaiah, M. Höök and M. Lindberg, *Proc. Natl. Acad. Sci. USA* **86**, 699 (1989)
25. J.A. Jones et al, *J. Biomol. NMR* **10**, 199 (1997)
26. M.K. Burnham et al, Patent, International Publication Number WO 94/18327 (1994)
27. C.J. Penkett, D. Phil. Thesis, University of Oxford (1997)
28. L. Mueller, *J. Magn. Reson.* **72**, 191 (1987)
29. M.J. McGavin, G. Raucci, S. Gurusiddappa and M. Höök, *J. Biol. Chem.* **266**, 8343 (1991)
30. M.J. McGavin, S. Gurusiddappa, P.E. Lindgren, M. Lindberg, G. Raucci and M. Höök, *J. Biol. Chem.* **268**, 23946 (1993)

